E-proceedings of the 36th IAHR World Congress
28 June – 3 July, 2015, The Hague, the Netherlands

FREE-SURFACE AND SEEPAGE BUBBLY FLOWS ON A GABION STEPPED SPILLWAY WEIR: EXPERIMENTAL OBSERVATIONS

GANGFU ZHANG[(1)], & HUBERT CHANSON[(2)]

[(1)] *The University of Queensland, School of Civil Engineering, Brisbane QLD 4072, Australia*
e-mail: gangfu.zhang@uqconnect.edu.au

[(2)] *The University of Queensland, School of Civil Engineering, Brisbane QLD 4072, Australia*
e-mail: h.chanson@uq.edu.au

ABSTRACT

Gabion stepped spillways are presented as a viable option for low to medium head designs. The material contributes to stability, low cost, flexibility, porosity and noise reduction. The steps also enhance energy dissipation, and reduce the requirement of a stilling basin. This paper constitutes a systematic study of the free-surface and seepage bubbly flows using a combination of phase-detection probe and high-speed video camera. The two-phase flow properties and turbulence characteristics in the free-surface flow were documented. The bubbly motion through the gabion material was analysed. The results demonstrated evidence of strong air-water mixing between the free-surface and seepage flows, and highlighted a modified cavity flow pattern as a result.

Keywords: *Gabion stepped spillways, Seepage flow, Air-water flow, Physical modelling*

1. INTRODUCTION

Stepped spillways have been used as flood release facilities for several centuries (Chanson 2002). The steps provide enhanced energy dissipation and reduce the need of a downstream stilling structure. The development of new construction techniques and materials in the past several decades has led to a regained interest in stepped spillway design and research.

The flow above a stepped spillway is highly turbulent (Rajaratnam 1990, Chanson and Toombes 2002). At low flows, the water cascades down the steps as a series of free-falling nappes (nappe flow regime). At intermediate flows, a transition flow takes place, and the flow appears chaotic with energetic droplet projections. At large discharges, the water skims over the pseudo-bottom formed by the step edges, and significant momentum exchange between the main and cavity flows takes place (skimming flow regime).

A distinctive feature of flow down a stepped spillway is the apparition of 'white water'. The turbulent stresses next to the air-water interface lead to uncontrolled air-entrainment in the forms of air bubbles and water droplets. This location is known as the inception point and cannot be exactly determined. The exchange between water and the atmosphere leads to intense air-water mixing, turbulence modulation and a complex flow pattern.

For low to medium head stepped weirs, the gabions may be a suitable construction material, which have the advantages of stability, low cost, flexibility, porosity and noise reduction (Agostini et al. 1987, Boes and Schmid 2003, Zhang and Chanson 2014). The flow patterns and energy dissipation performance on such spillways were investigated by Peyras et al. (1992) and Wuthrich and Chanson (2014). The additional porosity in the steps may result in a modified cavity recirculation pattern. The interactions between seepage and free-surface flow were discussed in Kells (1993).

Herein physical modelling was conducted to investigate the bubbly flow above a large scale 1V:2H gabion stepped spillway physical model. The two-phase flow properties in the mainstream, cavity and seepage flows were documented using a combination of dual-tip phase-detection probe measurements and high-speed video footage. The study aims to provide a detailed characterization of the turbulent air-water flow and highlight the interactions between seepage and cavity flow motions.

Figure 1. Gabion stepped weirs – Left: courtesy of Tony Marszalek; Right: courtesy of Officine Maccaferri

2. PHYSICAL MODELLING, EXPERIMENTAL FACILITY AND INSTRUMENTATION

2.1 Dimensional considerations

The complex turbulent air-water flow experienced above a stepped chute constitutes a great challenge in terms of physical modelling. On a stepped spillway, the dimensional analysis implies that relevant air-water flow properties must satisfy (Carosi and Chanson, 2006):

$$C, \frac{V}{V_c}, \frac{u'}{V_c}, \frac{F \times d_c}{V_c}, \ldots = F_1\left(\frac{x}{d_c}, \frac{y}{d_c}, \frac{d_c}{h}, \frac{q_W}{\sqrt{g \times h^3}}, \frac{\rho_W \times V \times D_H}{\mu_W}, \frac{g \times \mu_W^4}{\rho_W \times \sigma^3}, \frac{W}{d_c}, \theta, \frac{k_s'}{d_c}, Po \ldots\right) \quad [1]$$

where C is the void fraction, V is the interfacial velocity, u' is a characteristic turbulence velocity, F is the bubble count rate, d_c is the critical depth, V_c is the critical velocity, h is the step height, q_w is the discharge per unit width, D_H is the hydraulic diameter, x, y are the longitudinal and normal coordinates, ρ_w, μ_w are the density and dynamic viscosity of water, σ is the surface tension of water, W is the channel width, θ is the channel slope with respect to the horizontal, k_s' is the equivalent sand roughness, and Po the porosity of the gabion material. In Equation [1], the air-water flow properties at a given location are expressed as a function of dimensionless terms including the Froude, Reynolds and Morton numbers (4th, 5th and 6th terms).

For each configuration, the invariants were ρ_w, μ_w, g, σ, θ, k_s , h, and W. In turn the Morton number was an invariant. Equation [1] may be further simplified:

$$C, \frac{V}{V_c}, \frac{u'}{V_c}, \frac{F \times d_c}{V_c}, \ldots = F_1\left(\frac{x}{d_c}, \frac{y}{d_c}, \frac{d_c}{h}, \frac{q_w}{\sqrt{g \times h^3}}, \frac{\rho_w \times V \times D_H}{\mu_w}, \ldots\right) \quad [2]$$

Herein a Froude similitude was adopted based on Equation [2]. Note that a true dynamic similarity mandates all dimensionless numbers to be equal in both model and prototype, which could not be satisfied under current experimental conditions. The experiments were conducted in a large-size physical model operating at high Reynolds numbers to minimize any potential scale effects.

2.2 Experimental facility and instrumentation

New experiments were conducted in a large size gabion stepped weir physical model at the University of Queensland. The same facility was used by Wuthrich and Chanson (2014). The test section was 0.52 m wide and consisted of a broad-crested weir followed by 10 identical steps (h = 0.1 m, l = 0.2 m) made of gabion boxes. The gabions were 0.3 m long, 0.1 m high and 0.52 m wide, made of 14 mm sieved gravels. The gravel material had a dry density of 1.6 tonnes/m^3, a porosity of 0.35 – 0.4, and a hydraulic conductivity between 1.1 – 2.3 × 10^{-1} m/s. A photo of the experimental facility is provided in Figure 2.

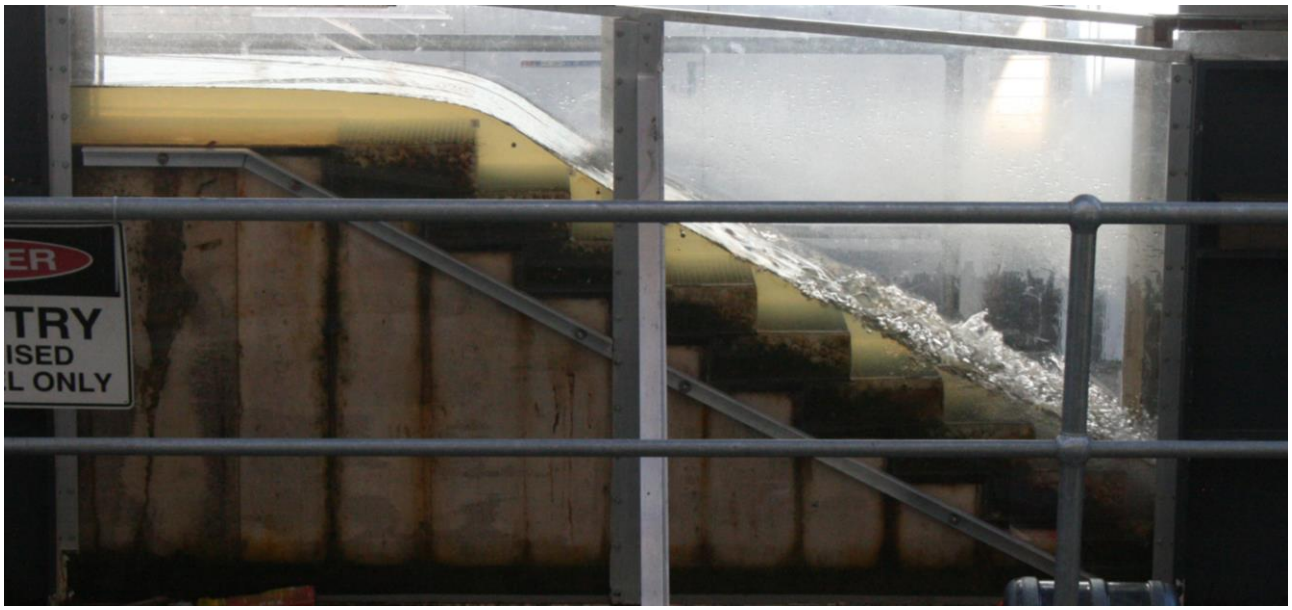

Figure 2. Gabion stepped spillway at the University of Queensland

The flow rate was deduced from total head measurement upstream of the test section using the calibration of Felder and Chanson (2012). Air-water properties in the overflow were recorded with a dual-tip phase-detection probe (Ø = 0.25 mm). The probe sensors were excited by an air bubble detector (AS25240) and scanned at 20 kHz per sensor for 45 s. The probe was mounted above a trolley which traversed along the channel centerline. The vertical movement was controlled by a fine adjustment travelling mechanism attached to a Mitutoyo™ digital scale with an accuracy of ±0.01 mm. The bubbly flow motion through the gabion material was documented using a combination of high shutter speed digital imagery (1/1,000 – 1/8,000 s) and high speed video recordings up to 1,000 fps (Casio™ EX-ZR200).

Flow rates between 0.052 and 0.147 m^2/s were investigated. Particular emphases were placed upon the transition and skimming flows which incorporated a rich amount of air. The flow patterns were observed through the perspex channel sidwalls. Air-water measurements were undertaken at the step edges and in the cavities. Bubble trajectories inside the gabion material were tracked at representative locations using a high speed video camera through the sidewall.

3. EXPERIMENTAL OBSERVATIONS

3.1 Presentation

Four distinct flow regimes were identified on the gabion stepped spillway, depending on the dimensionless discharge d_c/h where $d_c = (q^2/g)^{1/3}$ is the critical flow depth, and q is the flow rate per unit width. For very small discharges ($d_c/h < 0.2$), a porous flow regime was observed. The flow seeped from one gabion box to the next, leaving a short seepage face above each step tread which terminated before reaching the step edge. A fast water jet was seen shooting out from the last step rise to fulfill continuity. A slight increase in discharge above $d_c/h = 0.2$ resulted in water seeping through the step rise into the next gabion, and a further increase in discharge pushed the seepage line forward until a small amount of overflow occurred past the step edge.

For small discharges up to $d_c/h < 0.5$ to 0.6 a nappe flow regime was observed (Figure 3A). The gabions were saturated in the back and overflow occurred past the step edges. From a bystander's point of view, the flow resembled a series of free-falling nappes cascading down the stepped chute. Above the step tread a small water pool was present with a large ventilated cavity above, and no recirculation was observed. Similar findings were discussed by Wuthrich and Chanson (2014).

For $0.6 < d_c/h < 0.9$ a transition flow regime was observed. The overflow was characterized by strong turbulence coupled with vigorous droplet ejections and the free-surface appeared rough and irregular. The cavities were partially filled with alternating air cavity sizes from small to medium. A large amount of air was entrained in the downstream portion of the flow because of the extreme flow instability and turbulence.

For large discharges $d_c/h > 0.9$ a skimming flow was observed (Figure 3B). The upstream flow appeared smooth and glassy with approximately parallel streamlines. The inception point of free-surface aeration was well defined and clearly observable from the side of the channel. Downstream, the flow was dominated by a complex air-water mixing process and appeared highly turbulent. The step cavities were filled with a two-phase flow mixture, but contained a clear water core above the 1st third of the step tread, which was absent in conventional impervious stepped spillway structures (Matos 2001, Gonzalez and Chanson 2004).

(A) Nappe flow, $d_c/h = 0.27$, $Re = 5.6\times10^4$

(B) Skimming flow, $d_c/h = 1.2$, $Re = 5.2\times10^5$

Figure 3. Flow patterns above a gabion stepped weir

For all discharges, some air bubbles were transported in the seepage through the gabion materials. A characteristic two-phase flow pattern developed once the gabions became fully saturated (Figure 4A). Streams of air bubbles entered the gabion material through the downstream half of the step tread, below the region of shear layer impact above the step tread. Slow motion videos identified these as either individual or clusters of bubbles. The bubbly movement was fastest next to the step edge, and became subdued towards the back of the gabion material. The majority of air bubbles accelerated through the upper half of the step rise to enter the next step cavity, while a small number of bubbles recirculated down, back and upwards before returning to the cavity above. This typical pattern implied the existence of large positive pressure on the downstream end of the step tread and a subpressure zone next to the upper part of the step rise, consistent with pressure distributions recorded on impervious stepped faces (Sanchez-Juny et al. 2007).

A detailed examination of the video footages revealed bubbles recirculating, breaking up and coalescing in the gabion material. A broad spectrum of bubble sizes and shapes ranging from pseudo-ellipsoidal to highly distorted and elongated existed. The combination and constrictions of the gravels modified the shear stress distributions inside the gabion material, resulting in these processes to take place.

The bubbly movement highlighted some interactions between the overflow and seepage. Such interaction was most intense next to the step edge (Figure 4B). The majority of air bubbles were accelerated upwards and then in the streamwise direction immediately past the step rise, surrounding a clear water core formed above the first third of the step tread. Such a clear water core was previously reported for rough impervious steps (Gonzalez et al. 2008, Bung and Schlenkhoff 2010), but never for smooth impervious steps. The additional porosity allowed a reduction of form drag in the downstream cavity and caused the recirculating fluid to be modified compared to traditional impervious steps. This effect was known as ventilation and was documented in monophase flows (Naudascher and Rockwell 1994). Additionally, the step roughness may induce some turbulence manipulation in the developing boundary layer, similar to riblets and d-type roughness (Djenidi and Antonia 1995).

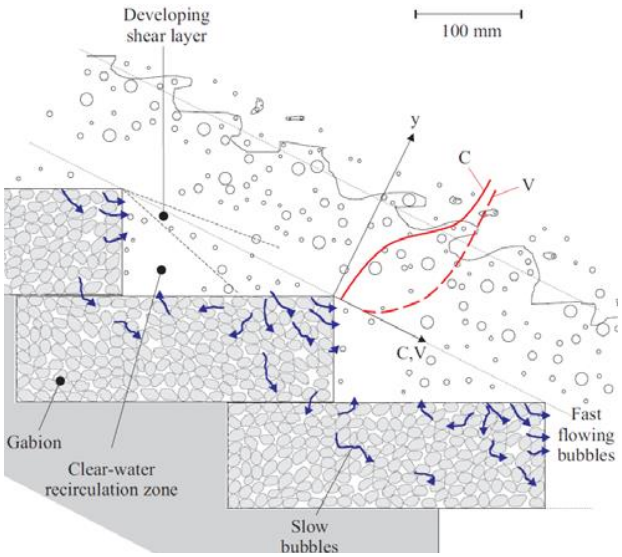

(A) Characteristic two-phase flow pattern

(B) Bubbly motion inside gabions – flow from left to right, 1/5,435 s

Figure 4. Two-phase skimming flow above a gabion stepped spillway

4. TWO-PHASE FLOW PROPERTIES

4.1 Free surface flow

On a stepped chute, the turbulence interactions next to the free-surface cause a large amount of air to be entrained. Downstream of the inception point, the void fraction profile above each step edge exhibited an inverted S-curve, typical of skimming flows (Chanson and Toombes 2002, Gonzalez and chanson 2008). Typical results are presented in Figure 5A, where C is the void fraction, y is the distance normal to the pseudo-bottom, and y_{90} is the height for C = 0.9. Comparison between the data and an analytical diffusion equation developed by Chanson and Toombes (2002) for skimming flows showed an excellent agreement. A subtle observation in Figure 5A is the non-zero void fraction at y = 0, resulting from the bubbly flux through the gabion materials.

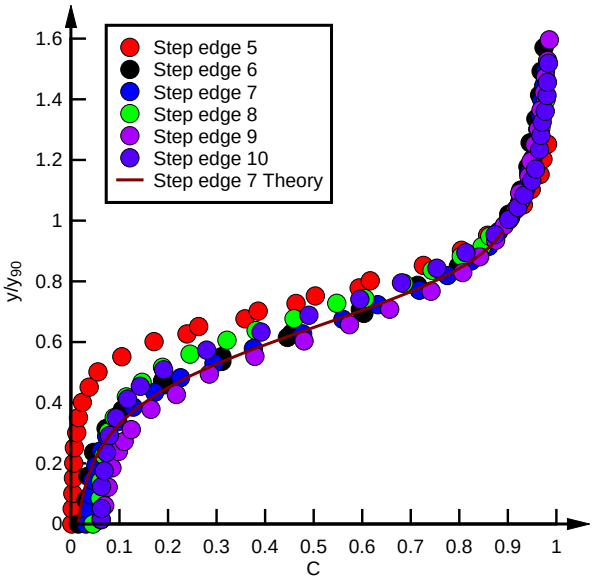

(A) Void fraction distributions - d_c/h = 1.0, Re = 4.0×10^5

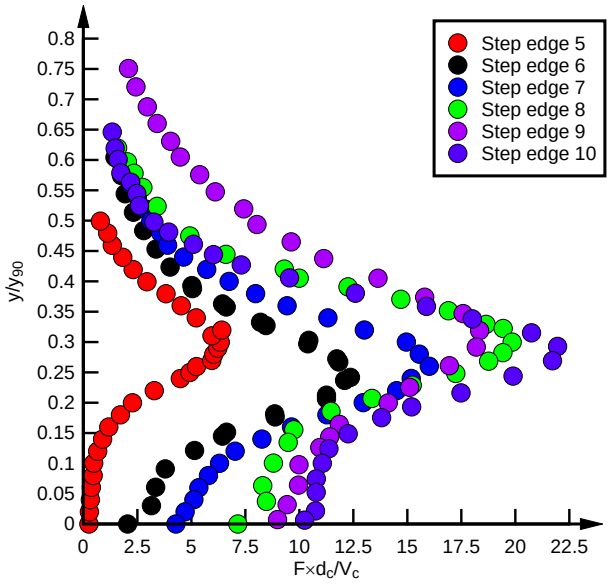

(B) Bubble count rate distributions – d_c/h = 1.0, Re = 4.0×10^5

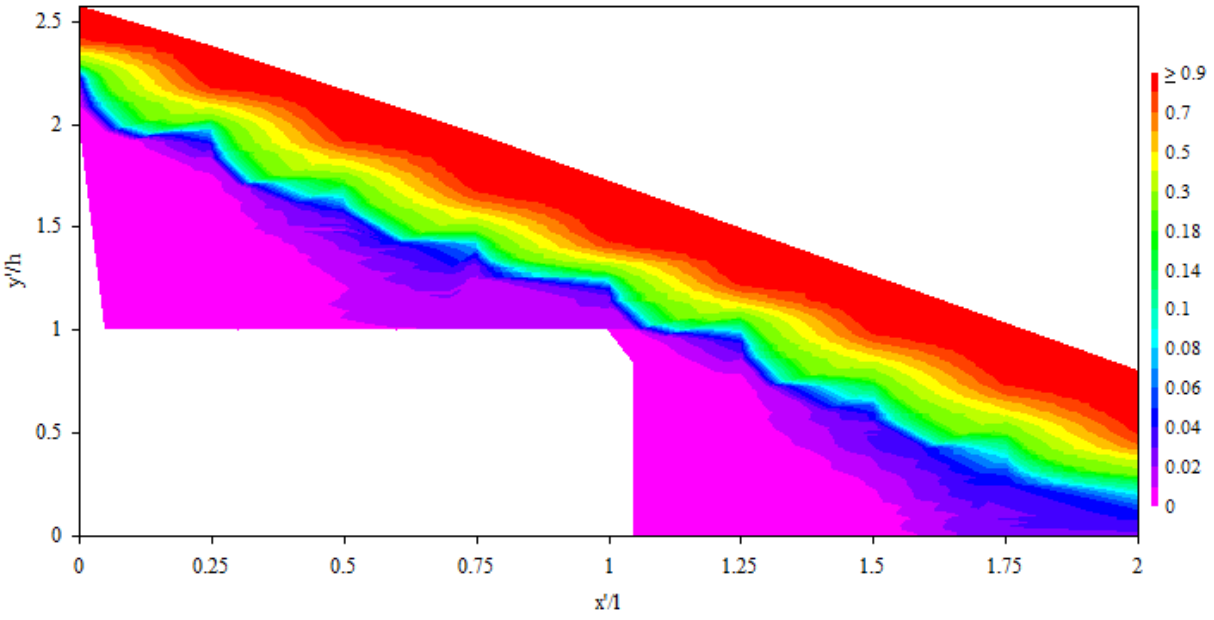

(C) Void fraction distribution inside step cavity – d_c/h = 1.3, Re = 5.9×10^5, step edges 7 - 9

Figure 5. Two-phase flow properties above a gabion stepped spillway

The bubble count rate F is defined as half the number of air-water interfaces detected by the probe sensor per second. For a given interfacial velocity, F is proportional to the specific interface area (Chanson 2002). Typical bubble count rate

distributions above the step edge are presented in dimensionless terms in Figure 5B, where $V_c = (g \times d_c)^{0.5}$ is the critical velocity. The data exhibited a distinct bell shape in the free-surface flow ($y > 0$), with a maximum value found in the mid-water column ($0.3 < y/y_{90} < 0.4$) corresponding to a void fraction about 0.4 – 0.5 as previously reported (Chanson and Toombes 2002, Felder and Chanson 2011).

Below the pseudo-bottom, both visual observations and phase-detection probe measurements indicated a drastically lesser extent of aeration. Typical void fraction distribution inside step cavities are presented in Figure 5C, where x' and y' are the distances along and normal to the step tread respectively. The data showed typical void fractions less than 10% below the pseudo-bottom and highlighted a clear water region above the first half of the step cavity, as discussed in Section 3.

The interfacial velocity (V) and turbulence intensity (Tu) distributions above step edges are presented in Figure 6 in dimensionless terms, where V_{90} is the velocity at $y = y_{90}$. Both data presented some self-similar shapes. The velocity profiles were modelled closely using a 1/10 power law, similar to some previous studies (e.g. Wuthrich and Chanson 2014). The shape of the velocity data highlighted a developing shear layer in the wake of the step edge (Figure 4A). The turbulence intensity is defined as the ratio between the standard deviation to the mean interfacial velocity, and was calculated based upon a cross-correlation technique between the probe signals (Chanson and Toombes 2002). The turbulent intensity value is reflective of the extent of turbulent fluctuations at different locations across the flow column. The maximum Tu value was typically recorded at $0.3 < y/d_c < 0.4$, close to the location of the maximum bubble count rate where $C \approx 0.5$. The location corresponded to approximately the middle of the shear layer. Overall larger turbulence levels were recorded above the last step edge (step edge 10), which may be linked with the interaction between the overflow and the increased seepage coming out of the last step rise.

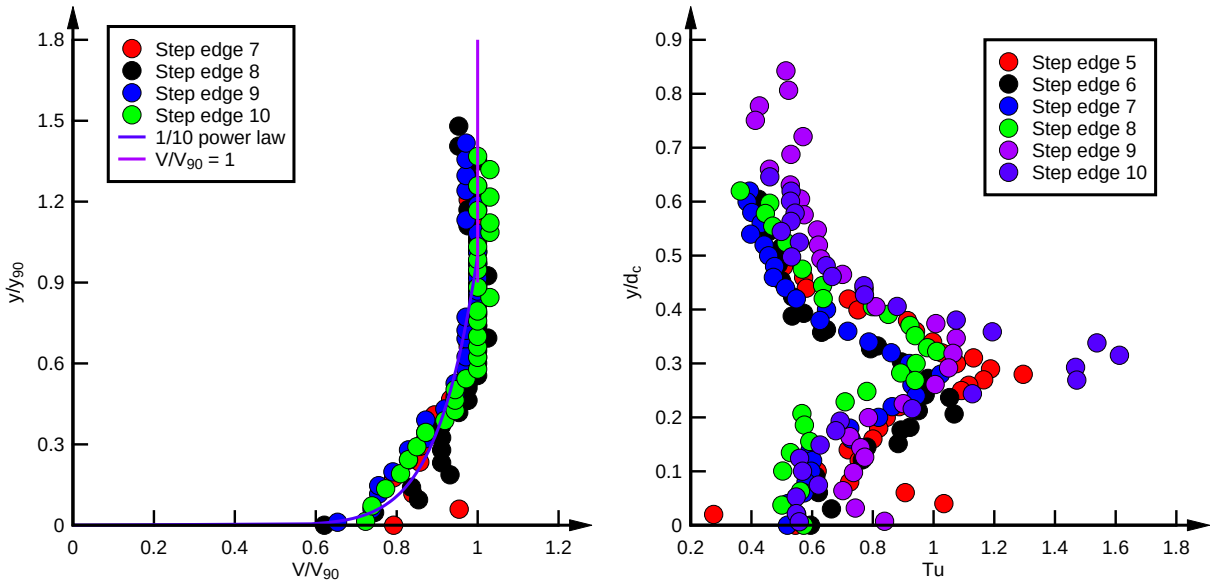

(A) Dimensionless velocity profiles – $d_c/h = 1.3$, $Re = 5.9 \times 10^5$ (B) Turbulence intensity profiles – $d_c/h = 1.0$, $Re = 4.0 \times 10^5$

Figure 6. Velocity and turbulence intensity profiles on a gabion stepped spillway

4.2 Seepage flow

High-speed movies were analysed to obtain the bubble trajectories, velocities and sizes in the gabion material. Figure 7 describes typical bubbly velocity distributions inside the gabion material, where X and Y are the horizontal and vertical coordinates respectively. The velocity analysis was repeated twice. In the first stage, each velocity vector was averaged over 20 (±1) bubbles. The results highlighted a region of significant bubbly motion next to the step corner (Figure 7). Maximum velocities up to 1 m/s were observed, with instantaneous velocities reaching 2 m/s. The average bubble velocities were smaller elsewhere inside the gabion, and were smallest below the step corner. The bubbles trajectories were typical for both transition and skimming flows, except below the step corner. In a skimming flow, the positive pressure on the first third of the step tread (i.e. clear water core) was large enough to drive some bubbles back into the previous gabion box, while in a transition flow they travelled forward in the flow direction. Some recirculation was also observed below the middle of the step, driven by an impacting shear layer above. Figure 7C illustrates the velocity distributions obtained in the second pass, where 100 (±5) bubbles were averaged to obtain each velocity vector. The seepage velocities accelerated in average through gabion boxes 6 – 8, and reached a maximum mean velocity of 0.8 m/s at step edge 8. The seepage next to the step edge appeared to accelerate more than elsewhere inside the gabion because of direct interaction with the spillway overflow. A close examination revealed subtly distinctive flow paths in different steps (step 7 vs 8). While this may be a result of physical constrictions (i.e. gravel layout etc), it may also be an indication of varying pressure distributions on the step faces, and that uniform equilibrium conditions were not achieved.

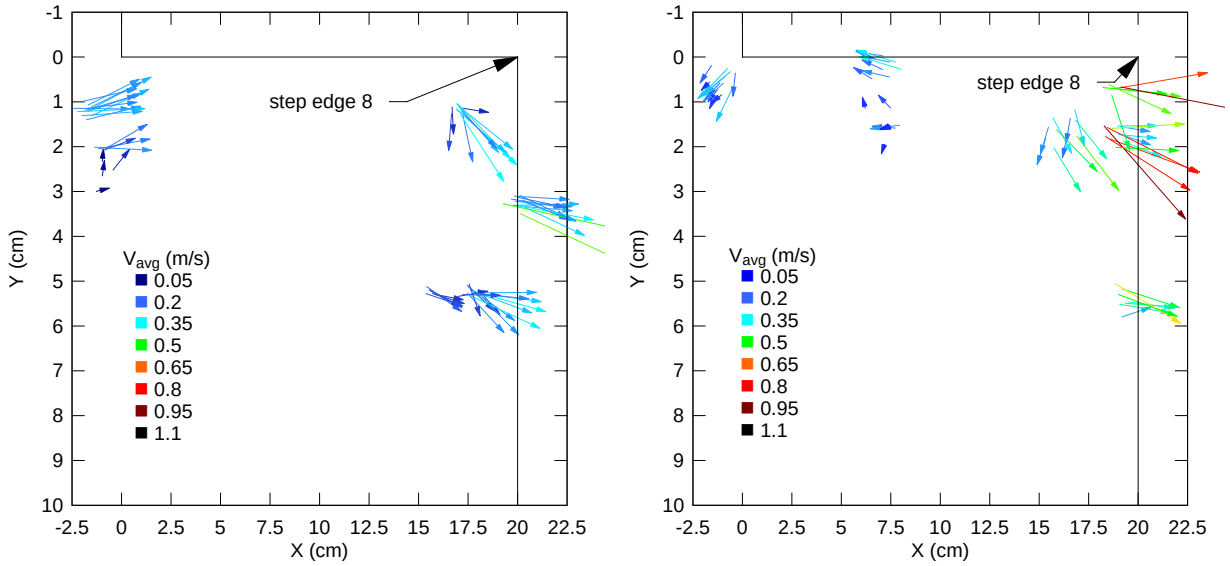

(A) Step 8, d_c/h = 0.7, Re = 2.3×10^5, average of 20±1 samples (B) Step 8, d_c/h = 1.3, Re = 5.9×10^5, average of 20±1 samples

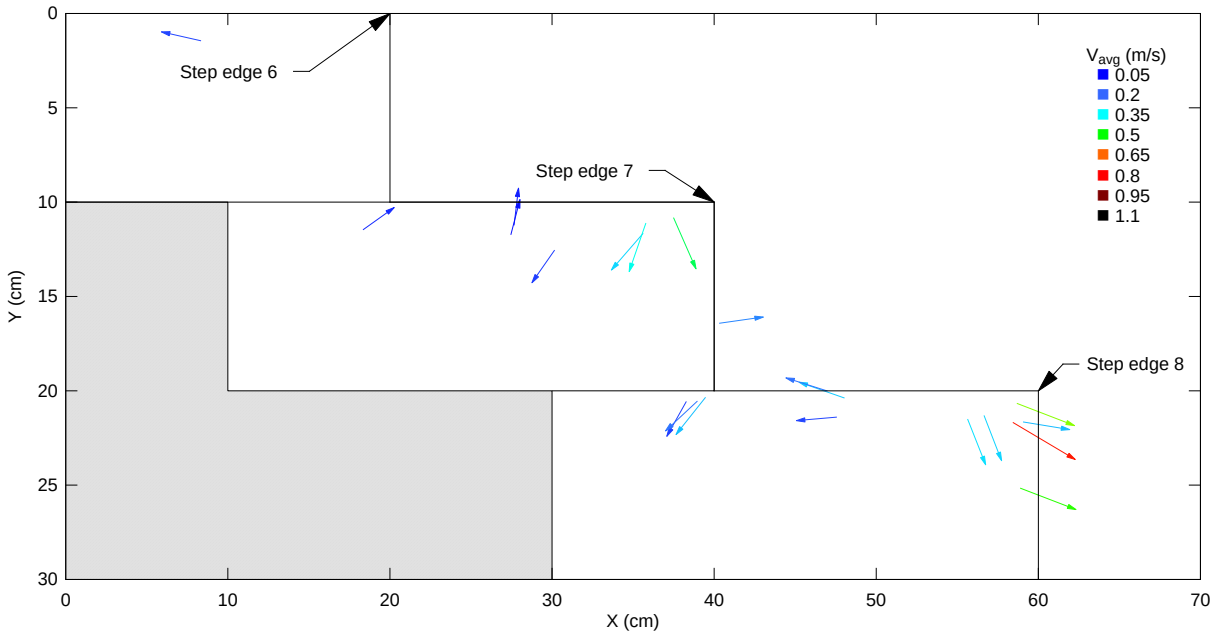

(C) Step 6-8, dc/h = 1.3, Re = 5.9×10^5, average of 100±5 samples

Figure 7. Average bubbly seepage velocity inside gabion material

The velocity fluctuations inside the gabion material are presented in Figure 8, in terms of the velocity differences (V_{75} – V_{25}) and (V_{90} – V_{10}), where the subscript denotes the velocity percentile. (V_{90} – V_{10}) and (V_{75} – V_{25}) are respectively the differences between the ninth and first deciles and between the third and first quartiles of the data ensemble. Assuming a Gaussian distribution, (V_{90} – V_{10}) and (V_{75} – V_{25}) would be equal to 2.66 and 1.3 times the standard deviation respectively. In Figure 8, the marker sizes are proportional to velocity fluctuations. The distribution of velocity fluctuations showed relatively large velocity fluctuations throughout the entire gabion materials, with the largest velocity fluctuations observed next to the step edges (up to 0.4 m/s). Lower quantitative values were observed below the step corner and deep inside the gabion box. In general, relatively higher levels of velocity fluctuations were recorded next to the gabion-cavity interfaces. The findings were consistent for both transition and skimming flows and agreed with visual observations. An increase in overflow discharge did only result in small change in velocity fluctuations.

Inside the gabions, the bubbles showed a variety of shapes and sizes caused by an unstable seepage motion coupled with interactions with the cavity fluid above. For a transition and a skimming flow rate, bubble sizes were deduced from detailed frame-by-frame video analyses with their distributions drawn in Figure 8. The bubbles were sampled across the entire gabion and their sizes were measured perpendicular to the seepage direction. For both flow regimes, Figure 9 recorded a skewed distribution with a preponderance of smaller bubble sizes. The dominant bubble size was between 0.6 and 0.9 mm in diameter. Visual observations also identified occasional occurrences of large bubbles (> 5mm) that were

mostly trapped in the interstitial gaps between gravels. The study ignored bubbles which coalesced or travelled in clusters.

A dispersion analysis was performed on the bubble trajectories next to step edge 8. Figure 10 plots the spatial deviations in the streamwise and normal directions as a function of elapsed time. A turbulent diffusion pattern was observed for $t\text{-}t_{start} < 0.01$ s, which may be simulated using a random walk model (Chanson 2004). Another combination of discharge, location, and layout of the gravels may result in a different dispersion pattern.

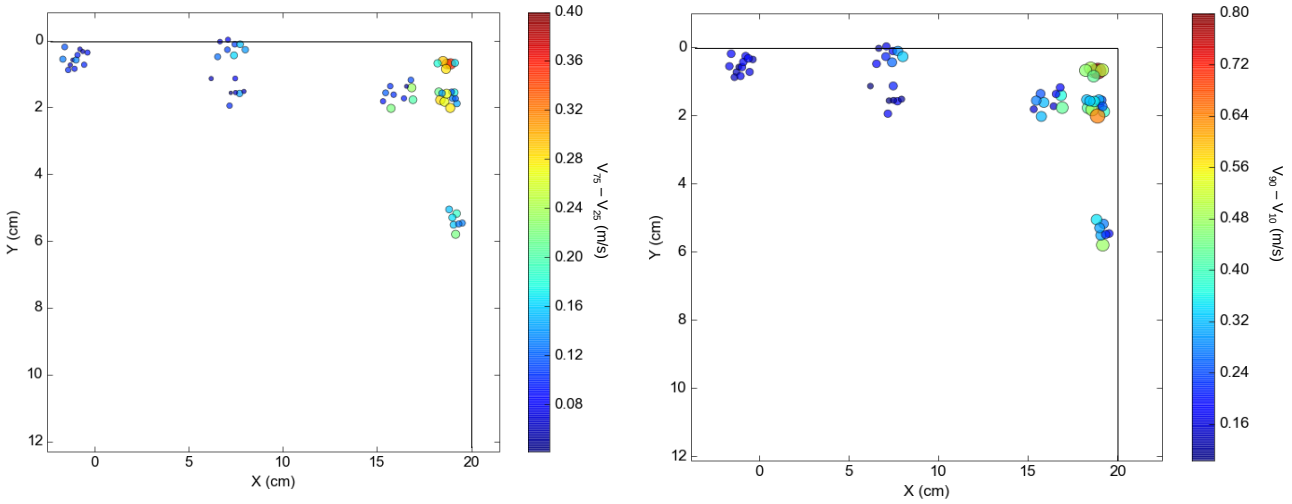

(A) $V_{75} - V_{25}$ (B) $V_{90} - V_{10}$

Figure 8. Velocity fluctuations in gabion box 8 – $d_c/h = 1.3$, $Re = 5.9\times10^5$

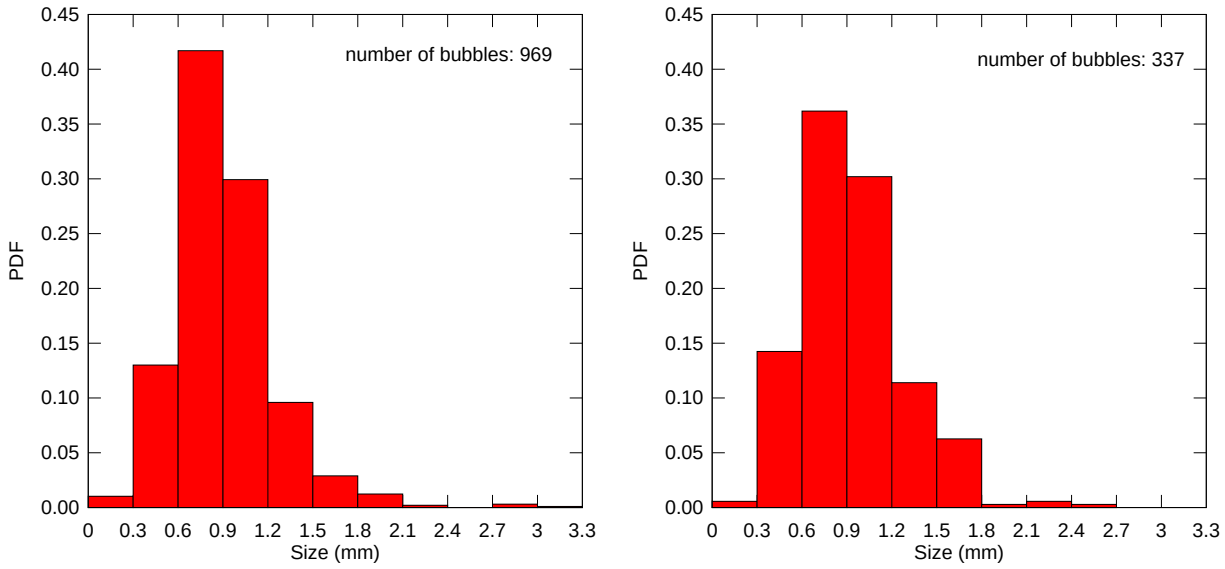

(A) $d_c/h = 0.7$, $Re = 2.3\times10^5$ (B) $d_c/h = 1.3$, $Re = 5.9\times10^5$

Figure 9. Bubbly size distributions in gabion materials

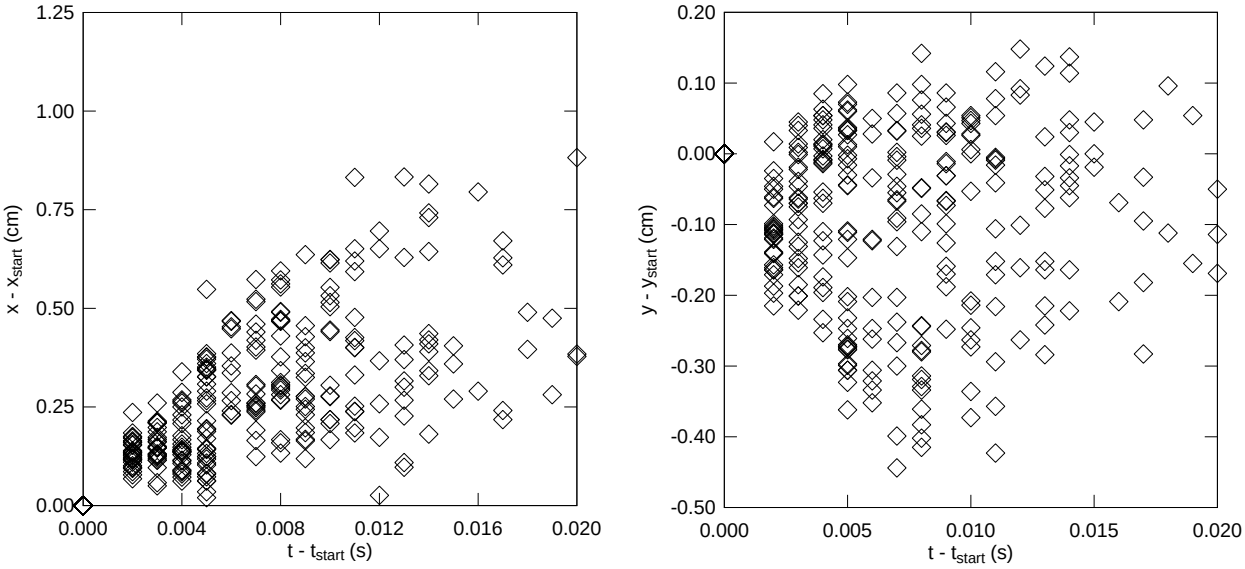

Figure 10. Spatial dispersion of air bubbles next to step edge 8 – d_c/h = 1.3, Re = 5.9×10^5

5. CONCLUSION

The free-surface and seepage bubbly flow on a gabion stepped weir was investigated. The two-phase flow properties were documented with a phase-detection probe in the overflow and high speed video movies in the gabion material. The results highlighted complex interactions between the free-surface and the atmosphere, and a modified cavity flow pattern resulting from the presence of seepage.

Quantitative measurements revealed strong air-water mixing in the overflow, in contrast to the drastically less aerated step cavities. The void fraction profiles matched an inverted S-shape predictable by theory, and the bubble count rates resembled a bell curve. The velocity profiles were closely modelled by a 1/10 power law and highlighted a developing shear layer in the wake of each step edge. The turbulence intensity profiles had maximum values in the mid-flow column, corresponding to locations of maximum bubble count rates.

High speed video analyses documented bubble trajectories as a function of the overflow discharge, flow regime, interstitial shape and location. Intense cavity-seepage interaction occurred on either side of the step edge, which was characterized by fast bubble velocities and large velocity fluctuations. Negative seepage was observed below the step corner in skimming flows, which may be a result of large positive pressures in the clear water core. Large positive and sub- pressures were identified above the downstream half of the step tread and in the wake of the step edge, corresponding to pressure distributions measured above impervious steps. The ventilation effect enhanced mixing between the free-surface and seepage flow, resulting in a complex cavity recirculation flow pattern. The air bubbles transported in the seepage were predominantly between 0.6 and 0.9 mm in diameter, and the diffusion process may be simulated with a random walk model.

6. ACKNOWLEDGEMENTS

The authors acknowledge the technical assistance of Jason Van de Gevel and Stewart Matthews. The financial support of Australian Research Council (Grant DP120100481) is acknowledged.

7. REFERENCES

Agostini, R., Bizzarri, A., Masetti, M., and Papetti, A. (1987). Flexible Gabion and Reno Mattress Structures in River and Stream Training Works. Section One: Weirs. Officine Maccaferri, Bologna, Italy, 2nd edition.

Bung, D.B., and Schlenkoff, A. (2010). Self-aerated Flow on Embankment Stepped Spillways - The Effect of Additional Micro-roughness on Energy Dissipation and Oxygen Transfer." Proc. 1st IAHR European Congress, 4-6 May, Edinburgh, Scotland, 6 pages (CD-ROM).

Carosi, G., and Chanson, H. (2006). Air-water time and length scales in skimming flow on a stepped spillway. Application to the spray characterisation. Report No. CH59/06, Division of Civil Engineering, The University of Queensland, Brisbane, Australia, July, 142 pages.

Chanson, H. (2001). The Hydraulics of Stepped Chutes and Spillways. Balkema, Lisse, The Netherlands, 418 pages.

Chanson, H. (2004). The Hydraulics of Open Channel Flow . An Introduction. Butterworth-Heinemann, 2nd edition, Oxford, UK, 630 pages.

Chanson, H., and Toombes, L. (2002). Air-Water Flows down Stepped chutes. Turbulence and Flow Structure Observations. International Journal of Multiphase Flow, Vol. 28, No. 11, pp. 1737-1761.

Djenidi, L., and Antonia, R. A. (1995). Riblet modelling using a second moment closure. Applied Science Research, Vol. 54, No. 4, pp. 249-266.

Felder, S., and Chanson, H. (2011). Air-Water Flow Properties in Step Cavity down a Stepped Chute. International Journal of Multiphase Flow, Vol. 37, No. 7, pp. 732–745.
Felder, S., and Chanson, H. (2012). Air-Water Flow Measurements in Instationary Free-Surface Flows. a Triple Decomposition Technique. Hydraulic Model Report No. CH85/12, School of Civil Engineering, The University of Queensland, Brisbane, Australia, 151 pages.
Gonzalez, C.A., and Chanson, H. (2004). Interactions between Cavity Flow and Main Stream Skimming Flows. an Experimental Study. Canadian Journal of Civil Engineering, Vol. 31, No. 1, pp. 33-44.
Gonzalez, C.A., Takahashi, M., and Chanson, H. (2008). An Experimental Study of Effects of Step Roughness in Skimming Flows on Stepped Chutes. Journal of Hydraulic Research, IAHR, Vol. 46, No. Extra Issue 1, pp. 24-35.
Kells, J.A. (1993). Spatially varied flow over rockfill embankments. Canadian Journal of Civil Engineering, Vol. 20, pp. 820-827.
Matos, J. (2001). Onset of skimming flow on stepped spillways - Discussion. Journal of Hydraulic Engineering-Asce, *127*(6), 519-521.
Naudascher, E., and Rockwell, D. (1994). Flow-induced vibrations. An engineering guide. IAHR Hydraulic Structures Design Manual No. 7, Balkema, The Netherlands.
Peyras, L., Royet, P. and Degoutte, G. (1992), Flow and energy dissipation over stepped gabion weirs, Journal of Hydraulic Engineering-ASCE, 118 (5), 707-717.
Rajaratnam, N. (1990). Skimming Flow in Stepped Spillways. Journal of Hydraulic Engineering, ASCE, Vol. 116, No. 4, pp. 587-591.
Sanchez-Juny, M.; Blade, E.; Dolz, J. (2007). Pressures on a stepped spillway. Journal of Hydraulic Research, Vol. 45, No. 4, pp. 505-511.
Wuthrich, D, and Chanson, H. (2014). Hydraulics, Air Entrainment and Energy Dissipation on Gabion Stepped Weir. Journal of Hydraulic Engineering, ASCE, Vol. 140, No. 9, Paper 04014046, 10 pages.
Zhang, G., and Chanson, H. (2014). Step Cavity and Gabion Aeration on a Gabion Stepped Spillway. Proceedings of the 5th IAHR International Symposium on Hydraulic Structures (ISHS2014), 25-27 June 2014, Brisbane, Australia, 8 pages.